CrossMark

Staurosporine-induced apoptotic water loss is cell- and attachment-specific

Michael A. Model[1] · Nathan J. Mudrak[1] · Priyanka S. Rana[1] · Robert J. Clements[1]

Abstract

Apoptotic volume decrease (AVD) is a characteristic cell shrinkage observed during apoptosis. There are at least two known processes that may result in the AVD: exit of intracellular water and splitting of cells into smaller fragments. Although AVD has traditionally been attributed to water loss, direct evidence for that is often lacking. In this study, we quantified intracellular water in staurosporine-treated cells using a previously described optical microscopic technique that combines volume measurements with quantitative phase analysis. Water loss was observed in detached HeLa and in adherent MDCK but not in adherent HeLa cells. At the same time, adherent HeLa and adherent MDCK cells exhibited visually similar apoptotic morphology, including fragmentation and activation of caspase-3. Morphological changes and caspase activation were prevented by chloride channel blockers DIDS and NPPB in both adherent and suspended HeLa cells, while potassium channel blocker TEA was ineffective. We conclude that staurosporine-induced dehydration is not a universal cell response but depends on the cell type and substrate attachment and can only be judged by direct water measurements. The effects of potassium or chloride channel blockers do not always correlate with the AVD.

Keywords Apoptotic volume decrease · Staurosporine · Intracellular water · Transport of intensity equation · Transmission-through-dye microscopy · Apoptotic bodies

Introduction

The remarkable and often the most noticeable feature of apoptosis is a decrease in cell size. While many other characteristics of apoptosis can be cell- and stimulus-dependent, shrinkage occurs very reliably. Numerous publications investigating various aspects of apoptotic volume decrease (AVD) have appeared in the 1990–2000s and resulted in significant progress in our understanding of this phenomenon [1–4].

Volume decrease in apoptotic cells can occur both by water loss and by fragmentation; of these, the first mechanism has received most attention. The most popular model of the AVD envisions activation of K^+ and/or Cl^- channels causing a loss of intracellular ions and osmotically-driven water efflux. In many cases, blockers of K^+ or Cl^- channels

applied simultaneously with an apoptotic stimulus prevent both shrinkage and all other manifestations of apoptosis.

Fragmentation and generation of smaller apoptotic bodies is another typical sign of apoptosis; it has been documented on numerous micrographs and by light scatter [5]. In addition to formation of small particles, the cells from which those particles have separated are also supposed to become smaller. When the total cell volume is the only measured parameter, there is not enough information to unequivocally attribute volume decrease to dehydration or to fragmentation.

There have been relatively few publications where cell dry mass or water content have been measured directly. The most convincing data come from buoyant density measurements [6–10]. At the same time, not all density centrifugation experiments agree with the dehydration model of the AVD [11, 12]. Other authors have reported a decrease in the phase delay of light passing through the cell, which can only be interpreted as a reduction in the cells' dry mass [13–17]. Thus, it appears that both factors may in principle contribute to what is known as the AVD.

✉ Michael A. Model
  mmodel@kent.edu

[1] Department of Biological Sciences, Kent State University, Kent, OH 44242, USA

In this work, we applied a recently described microscopic method [18] to quantify water loss in apoptosis induced by a protein kinase inhibitor staurosporine (ST). ST has been a popular apoptosis inducer for studying AVD and related ion changes [19–27]. In particular, two publications from the Okada group [19, 28] reported a volume decrease in detached HeLa cells stimulated with ST as measured on an electronic size analyzer. We replicated the conditions employed by these authors, but measured intracellular water instead of the volume; a pronounced water loss has indeed been observed. At the same time, when HeLa cells were attached to glass, ST caused no loss of water; this was all the more remarkable since the cells were undergoing dramatic shape changes and fragmentation. To see if the lack of ST-induced water loss is a general characteristic of adherent cell lines, we tested ST on Madin-Darby Canine Kidney (MDCK) cells. MDCK responded with morphological changes that were very similar to those exhibited by HeLa but, unlike HeLa, they quickly became dehydrated. We conclude that the specific mode of action of ST depends on the cell type and on the state of attachment. To make conclusions about water loss, accurate water measurements are necessary.

Methods

Cell culture and treatment

HeLa and MDCK cells (ATCC, Manassas, VA) were grown in DMEM medium (Lonza) with 10% FBS and antibiotics. For microscopic observation of adherent cultures, cells were transferred to No. 1.5 coverslips or to coverslip-bottom chambers (Ibidi, Martinsried, Germany) no later than 24 h before the experiment. Measurements of intracellular water content were done as described previously [18]. Approximately 10–15 min before imaging, the medium was replaced with an identical one containing additionally 7 mg/ml Acid Blue 9 (AB9) (TCI America, Portland, OR), and the coverslips were mounted on slides over small spots of silicone grease [29]. When monitoring adherent HeLa over prolonged periods, coverslips were continuously kept in DMEM/AB9; the presence of the dye does not affect cell viability and functioning [18, 30, 31]. To prepare suspended HeLa samples, cells were detached from culture dishes using trypsin and transferred into fresh DMEM at 2.5×10^6 cells/ml. They were incubated with agitation on a battery-operated platform for 2 h in a 5% CO_2 atmosphere before treatment (in that, we followed the previously published protocol of Hazama and Okada [19, 32]). Prior to intracellular water measurements, the cells were centrifuged and resuspended in DMEM/AB9; the absorption of the final solution was determined by the lens-immersion method [33].

Apoptosis was induced with 2 µM ST (Cayman Chemical, Ann Arbor, MI). In some experiments, stimulation with ST was carried out in the presence of ion channel blockers: 10 mM of potassium blocker tetraethylammonium chloride (TEA, Sigma-Aldrich, St. Louis, MO), or 0.5 mM of chloride blockers 4,4′-diisothiocyanato-2.2′-stilbenedisulfonic acid (DIDS) or 5-nitro-2-(3-phenylpropylamino)benzoic acid (NPPB; both from Cayman).

Microscopy and sample analysis

Individual cell protein concentration was determined by transport-of-intensity (TIE) imaging with parallel volume measurements by the dye exclusion method (transmission-through-dye or TTD) [18, 29, 30, 34, 35]. The samples were imaged on an Olympus IX81 microscope (Olympus, Center Valley, PA) in transmitted light. First, two images were collected through a 485 nm band-pass filter: one in focus and the other by shifting the focal plane 5 µm into the sample; these two images allow the computation of the phase delay of transmitted light from the TIE equation; the output of the TIE had been previously calibrated in units of dry mass M_{dry} [18]. Observation of the same sample through a 630 nm filter gives the cell volume from displacement of the strongly absorbing dye AB9 by the cells. By dividing the dry mass by the cell volume, intracellular macromolecular concentration is obtained:

$$C \text{ (g/ml)} = M_{dry}(pg)/V(mm^3)$$

Conversion of protein concentration C (g/ml) into the volume fraction occupied by water (W) was done as

$$W = 1 - 0.70 \, C$$

which is based on the typical value for protein density, 1.4 g/ml [36]. This operation does not necessarily have to be performed on entire individual cells: parts of cells or, conversely, large cell clusters are equally suitable.

To detect apoptosis, we used 5 µM of the CellEvent reagent (ThermoFisher) for visualizing activated caspase-3/7 and 1,1′,3,3,3′,3′-hexamethylindodicarbocyanineiodide (DiIC$_1$(5), Anaspec, Fremont,CA) for mitochondrial membrane potential. The cells were imaged on an Olympus confocal microscope FV1000 using 488 nm excitation for CellEvent and 635 nm for DiIC$_1$(5). Flow cytometric analysis of CellEvent and DiIC$_1$(5) staining was performed on a FacsAria flow cytometer (BD Biosciences, San Jose, CA) using excitation at 488 and 635 nm, respectively.

Results

Adherent HeLa cells undergo apoptosis without water loss

Cells treated with staurosporine quickly begin to form slender and loosely bound processes (Fig. 1a, b). Because the exact cell boundaries are now hard to determine, cell water content becomes a more reliable metric than the volumes of individual cells.

Figure 2 shows the results of water measurements pooled from twelve separate experiments. The data were consistent and showed no major or persistent water loss. At the same time, staining for caspase 3/7 and mitochondrial membrane potential confirmed that apoptosis was indeed stimulated by staurosporine treatment (Fig. 3).

## Suspended HeLa cells undergo apoptosis accompanied by water loss

The observed lack of volume decrease was at variance with the much-cited publication by Maeno et al. [19]. Those authors, however, used HeLa cells detached from the plate and kept in suspension. Therefore, we attempted to replicate their conditions: HeLa were trypsinized, transferred to fresh medium and kept in suspension for two hours before applying ST. There was a clear loss of intracellular water under these conditions (Table 1), which agrees with the notion that staurosporine-induced shrinkage results from dehydration. The scatter in the data for dry mass was much greater than for W, and we did not attempt to analyze enough cells to conclude whether there was also a concomitant loss of organic matter (for example, because of fragmentation) in addition to water loss.
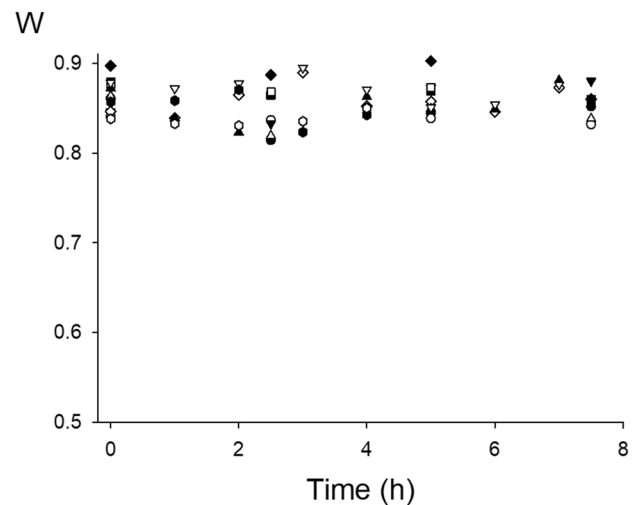
Fig. 2 Relative volume occupied by water during incubation of adherent HeLa cells with staurosporine. Different symbols indicate data obtained in different experiments; each symbol represents the average water content for multiple groups containing from 2 to 17 cells. The average water content $W = 0.857$ corresponds to the protein concentration of 0.205 g/ml, which agrees with our previous data [18] and lies within the typical range for mammalian cells [37, 38]

Apoptosis in adherent MDCK cells involves water loss

Next, we tested whether the lack of staurosporine-induced dehydration is a general property of attached cells. MDCK cells respond to staurosporine with morphological and biochemical changes similar to those of attached HeLa (Figs. 1c, 3); but, unlike HeLa, they showed a substantial loss of water (Table 1).
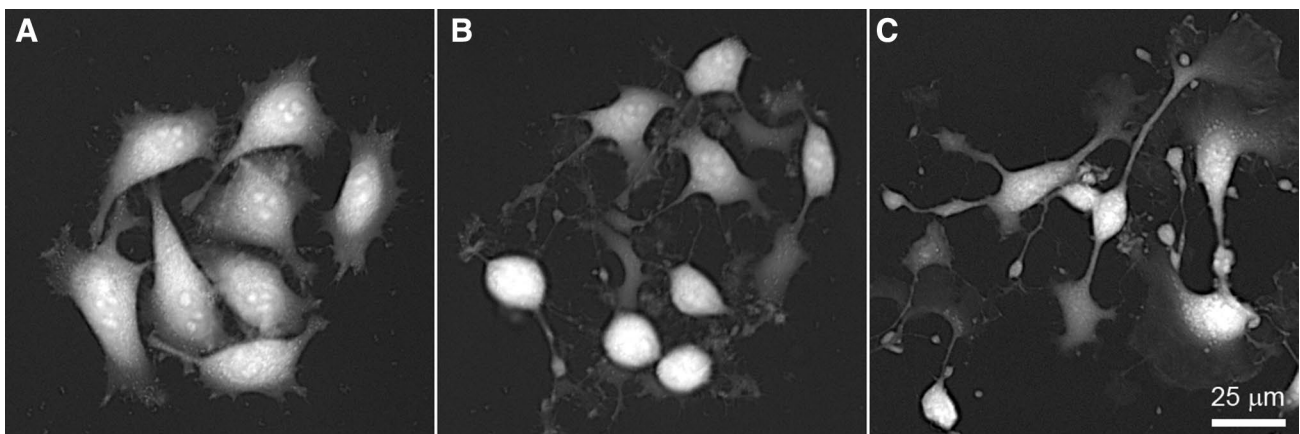
Fig. 1 **a, b** TTD images of the same population of HeLa cells before and 1 h after addition of staurosporine. **c** MDCK cells treated with staurosporine. Cell brightness in TTD images is directly proportional to local thickness

Fig. 3 Caspase (green) and mitochondrial potential staining by $DiIC_1(5)$ (red) of HeLa and MDCK cells. Cells were either exposed to 2 µM staurosporine for 8 h or left untreated. No caspase activation was noted after 2 h of treatment (not shown). (Color figure online)
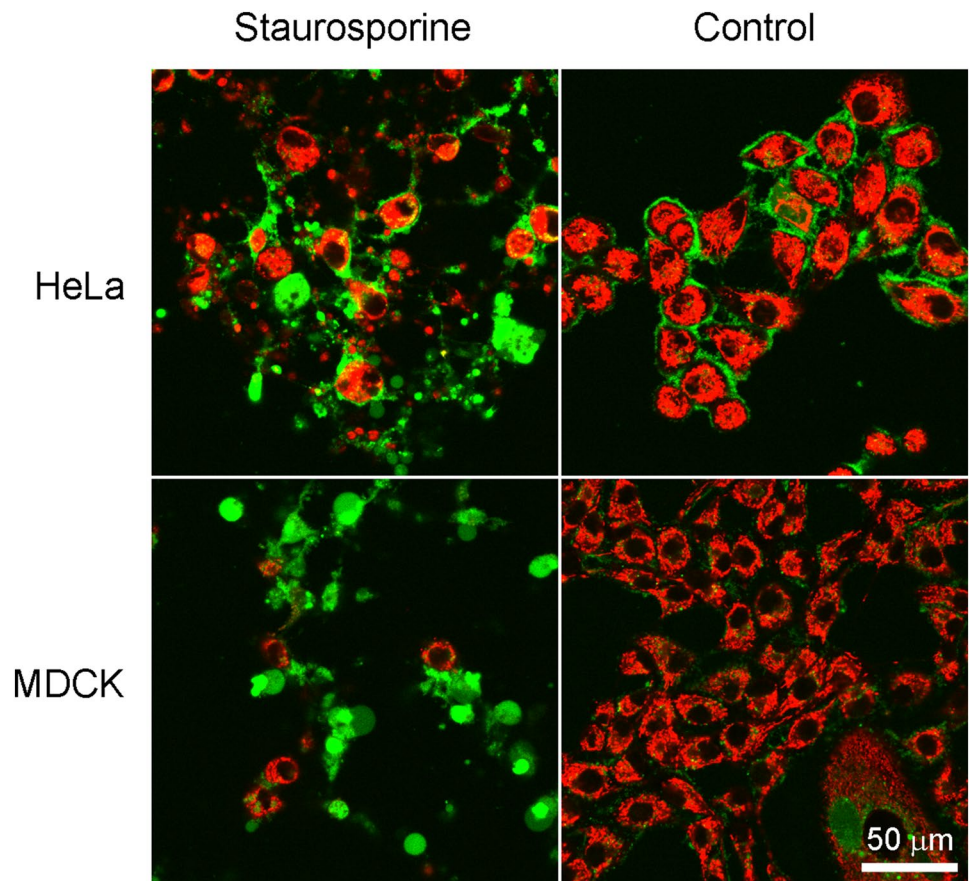
Table 1 Water and dry mass measurements in staurosporine-treated cells

	HeLa in suspension		MDCK adherent	
	Experiment 1	Experiment 2	Experiment 1	Experiment 2
Control				
W	0.825 ± 0.009 (61)	0.832 ± 0.009 (34)	0.869 ± 0.016 (39)	0.879 ± 0.007 (47)
M_{dry}, pg	626 ± 114	634 ± 94		
Staurosporine				
W	0.782 ± 0.017 (68)	0.798 ± 0.007 (74)	0.800 ± 0.024 (44)	0.792 ± 0.067 (33)
M_{dry}, pg	661 ± 59	656 ± 56		

Incubation with ST was carried out for 4 h for HeLa and 1.5 h for MDCK. The differences between W in staurosporine-treated and control cells was statistically significant with $P < 10^{-3}$; the differences in M_{dry} were insignificant

The effect of inhibitors

In the publication by Maeno et al. [19], apoptosis in suspended HeLa cells was prevented by chloride channel blockers DIDS and NPPB. We have repeated some of their experiments with a similar outcome (Fig. 4a): both DIDS and NPPB prevented caspase activation, although NPPB allowed depolarization of mitochondria. The potassium channel blocker TEA failed to suppress apoptosis (in the cited work, no experiments with TEA were reported). Adherent HeLa responded to channel blockers in the same way as they did

in suspension: DIDS and NPPB, but not TEA, prevented ST-induced morphological changes and caspase activation (Fig. 4b).

Discussion

Water loss does not always have to be equivalent to volume decrease, and it is likely that in some reports of the AVD, cell fragments were mistaken for shrunken and dehydrated cells [4, 36]. This kind of ambiguity can be avoided by using
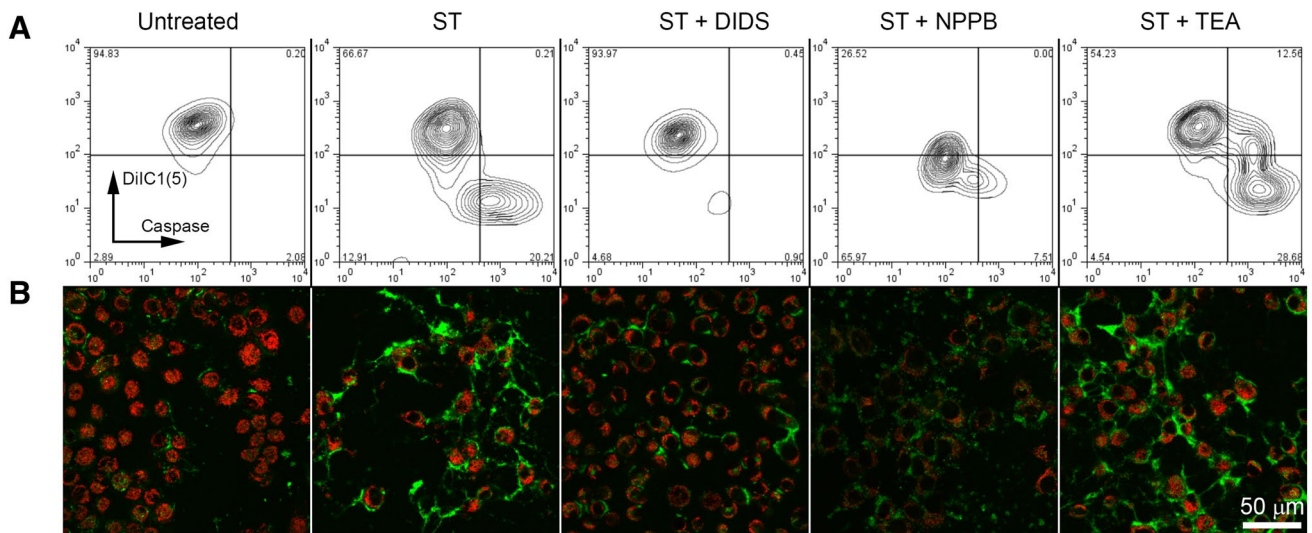
Fig. 4 The effect of channel blockers on suspended and attached HeLa. **a** Flow cytometric data for suspended cells stained with CellEvent (horizontal) and $DiIC_1(5)$ (vertical). **b** Confocal fluorescence images of attached cells, with CellEvent staining displayed in green and $DiIC_1(5)$ in red. Incubations with ST and inhibitors were carried out for 6 h. Because our results with suspended cells were similar to the previously published ones [19], we only provide single representative FACS plots. (Color figure online)

combined TIE/TTD microscopy, which quantifies dry mass and intracellular water separately from the total volume. The method is effective even when individual cells are difficult to measure, as is the case with spread and splintered staurosporine-treated cells.

We re-examined the effect of ST on suspended HeLa cells, where a decrease in the average cell volume was previously interpreted as dehydration [19]. By using direct measurements of intracellular water, we came to the same conclusion.

Attached HeLa cells behaved differently. Despite the rapid development of dramatic morphological changes, intracellular water remained constant for at least 8 h. This was not due to suppression of other markers of apoptosis, because caspase activation and depolarization of mitochondria were quite pronounced by that time. We wish to point out that the multiple cell protuberances, most of which remain attached to parent cells while in adherent state (Fig. 1b, c), become separated during trypsinization (not shown). Thus, if adherent and ST-treated cells were detached and ran on a particle analyzer or on a flow cytometer, one might have concluded that that the cells underwent AVD.

The lack of dehydration in adherent ST-stimulated cells prompted us to ask whether this could be a general feature of adherent cultures. The answer to this question was negative because MDCK cells, whose visible appearance under ST treatment was very similar to that of HeLa (Fig. 1), became dehydrated after 2 h of treatment.

We tested some of the ion channel blockers that prevented cell death in HeLa suspensions [19]. The chloride blockers DIDS and NPPB abolished apoptosis in both attached and

suspended HeLa, even though attached HeLa exhibited no water loss. Thus, their effects may be unrelated to chloride channels and the AVD: direct inhibition of caspases [39] or activation of the PI3K/Akt signaling by DIDS [40] may be the explanation. Likewise, the action of NPPB can extend beyond chloride channels [41, 42]. No protective effect of potassium blocker TEA was noted. The conclusion from this part of the study was that the effect of some ion channels blockers on apoptosis may not correlate with water loss.

One additional observation can be made. If water loss were the only factor in shrinkage, the relative volume change would be

$$\left(\frac{V_2}{V_1}\right)_W = \frac{1 - W_1}{1 - W_2}$$

where the subscripts 1 and 2 refer to the initial and shrunken stages. On the other hand, it follows from the conditions of electrical neutrality and osmotic equilibrium that when the volume decrease is caused solely by an efflux of K^+ and Cl^- at a constant pH, the maximum extent of shrinkage (at complete depletion of Cl^-) would be

$$\left(\frac{V_2}{V_1}\right)_W = 1 - \frac{2[Cl]_1}{P}$$

where P stands for external osmolarity [4]. The measured W in apoptotic MDCK cells corresponds to $(V_2/V_1)_w$ between 0.60 and 0.66; assuming that intracellular chloride concentration in these cells is 60 mM [43], these values are close to the chloride-imposed limit.

References

1. Bortner CD, Cidlowski JA (2002) Apoptotic volume decrease and the incredible shrinking cell. Cell Death Differ 9:1307–1310

2. Bortner CD, Cidlowski JA (2004) The role of apoptotic volume decrease and ionic homeostasis in the activation and repression of apoptosis. Pflugers Arch 448:313–318

3. Orlov SN, Platonova AA, Hamet P, Grygorczyk R (2013) Cell volume and monovalent ion transporters: their role in cell death machinery triggering and progression. Am J Physiol Cell Physiol 305:C361–C372

4. Model MA (2014) Possible causes of apoptotic volume decrease: an attempt at quantitative review. Am J Physiol Cell Physiol 306:C417–C424

5. McCarthy JV, Cotter TG (1997) Cell shrinkage and apoptosis: a role for potassium and sodium ion efflux. Cell Death Differ 4:756–770

6. Cohen GM, Sun XM, Snowden RT, Dinsdale D, Skilleter DN (1992) Key morphological features of apoptosis may occur in the absence of internucleosomal DNA fragmentation. Biochem J 286:331–334

7. Yamada T, Ohyama H (1988) Radiation-induced interphase death of rat thymocytes is internally programmed (apoptosis). Int J Radiat Biol Relat Stud Phys Chem Med 53:65–75

8. Wyllie AH, Morris RG (1982) Hormone-induced cell death. Purification ad properties of thymocytes undergoing apoptosis after glucocorticoid treatment. Am J Pathol 109:78–87

9. Patterson SD, Grossman JS, D'Andrea P, Latter GI (1995) Reduced numatrin/B23/nucleophosmin labeling in apoptotic Jurkat T-lymphoblasts. J Biol Chem 270:9429–9436

10. Grover WH, Bryan AK, Diez-Silva M, Suresh S, Higgins JM, Manalis SR (2011) Measuring single-cell density. Proc Natl Acad Sci 108:10992–10996

11. Benson RS, Heer S, Dive C, Watson AJ (1996) Characterization of cell volume loss in CEM-C7A cells during dexamethasone-induced apoptosis. Am J Physiol 270:C1190–C1203

12. Yurinskaya V, Goryachaya T, Guzhova I, Moshkov A, Rozanov Y, Sakuta G, Shirokova A, Shumilina E, Vassilieva I, Lang F, Vereninov A (2005) Potassium and sodium balance in U937 cells during apoptosis with and without cell shrinkage. Cell Physiol Biochem 16:155–162

13. Khmaladze A, Matz RL, Epstein T, Jasensky J, Banaszak Holl MM, Chen Z (2012) Cell volume changes during apoptosis monitored in real time using digital holographic microscopy. J Struct Biol 178:270–278

14. Khmaladze A (2017) Examining live cell culture cultures during apoptosis by digital holographic phase imaging and Raman spectroscopy. J Phys Conf Ser 909:012001

15. Mugnano M, Calabuig A, Grilli S, Miccio L, Ferraro P (2015) Monitoring cell morphology during necrosis and apoptosis by quantitative phase imaging. Proc SPIE 9529:952901–952909

16. Sharikova A, Saide G, Sfakis L, Park JY, Desta H, Maloney MC, Castracane J, Mahajan SD, Khmaladze A (2017) Monitoring of live cell cultures during apoptosis by phase imaging and Raman spectroscopy. Proc SPIE 10074:100740V–100740V1

17. Zhang Q, Zhong L, Tang P, Yuan Y, Liu S, Tian J, Lu X (2017) Quantitative refractive index distribution of single cell by combining phase-shifting interferometry and AFM imaging. Sci Rep 7:2532

18. Mudrak NJ, Rana PS, Model MA (2017) Calibrated brightfield-based imaging for measuring intracellular protein concentration. Cytometry 93:297–304

19. Maeno E, Ishizaki Y, Kanaseki T, Hazama A, Okada Y (2000) Normotonic cell shrinkage because of disordered volume regulation is an early prerequisite to apoptosis. Proc Natl Acad Sci USA 97:9487–9492

20. Krumschnabel G, Maehr T, Nawaz M, Schwarzbaum PJ, Manzl C (2007) Staurosporine-induced cell death in salmonid cells: the role of apoptotic volume decrease, ion fluxes and MAP kinase signaling. Apoptosis 12:1755–1768

21. l'Hoste S, Chargui A, Belfodil R, Corcelle E, Duranton C, Rubera I, Poujeol C, Mograbi B, Tauc M, Poujeol P (2010) CFTR mediates apoptotic volume decrease and cell death by controlling glutathione efflux and ros production in cultured mice proximal tubules. Am J Physiol Renal Physiol 298:F435–F453

22. Arrebola F, Cañizares J, Cubero MA, Crespo PV, Warley A, Fernández-Segura E (2005) Biphasic behavior of changes in elemental composition during staurosporine-induced apoptosis. Apoptosis 10:1317–1331

23. Krick S, Platoshyn O, McDaniel SS, Rubin LJ, Yuan JX (2001) Augmented K^+ currents and mitochondrial membrane depolarization in pulmonary artery myocyte apoptosis. Am J Physiol Lung Cell Mol Physiol 281:L887–L894

24. Wible BA, Wang L, Kuryshev YA, Basu A, Haldar S, Brown AM (2002) Increased K^+ efflux and apoptosis induced by the potassium channel modulatory protein KChAP/PIAS3β in prostate cancer cells. Biol Chem 277:17852–17862

25. Porcelli AM, Ghelli A, Zanna C, Valente P, Ferroni S, Rugolo M (2004) Apoptosis induced by staurosporine in ECV304 cells requires cell shrinkage and upregulation of Cl- conductance. Cell Death Differ 11:655–662

26. Yurinskaya VE, Rubashkin AA, Vereninov AA (2011) Balance of unidirectional monovalent ion fluxes in cells undergoing apoptosis: why does Na^+/K^+ pump suppression not cause cell swelling? J Physiol 589:2197–2211

27. O'Reilly N, Xia Z, Fiander H, Tauskela J, Small DL (2002) Disparity between ionic mediators of volume regulation and apoptosis in N1E 115 mouse neuroblastoma cells. Brain Res 943:245–256

28. Dezaki K, Maeno E, Sato K, Akita T, Okada Y (2012) Early-phase occurrence of K^+ and Cl^- efflux in addition to Ca^{2+} mobilization is a prerequisite to apoptosis in HeLa cells. Apoptosis 17:821–831

29. Model MA (2015) Cell volume measurements by optical transmission microscopy. Curr Protoc Cytom 72:12.39.1–12.39.9

30. Gregg JL, McGuire KM, Focht DC, Model MA (2010) Measurement of the thickness and volume of adherent cells using transmission-through-dye microscopy. Pflugers Arch 460:1097–1104

31. Kasim NR, Kuželová K, Holoubek A, Model MA (2013) Live fluorescence and transmission-through-dye microscopic study of actinomycin D-induced apoptosis and apoptotic volume decrease. Apoptosis 18:521–532

32. Hazama A, Okada Y (1988) Ca^{2+} sensitivity of volume-regulatory K^+ and Cl^- channels in cultured human epithelial cells. J Physiol 402:687–702

33. Model MA, Khitrin AK, Blank JL (2008) Measurement of the absorption of concentrated dyes and their use for quantitative imaging of surface topography. J Microsc 231:156–167

34. Model MA (2012) Imaging the cell's third dimension. Microsc Today 20:32–37

35. Gibbons BA, Robinson LC, Kharel P, Synowicki RA, Model MA (2016) Volume measurements and fluorescent staining indicate an increase in permeability for organic cation transporter substrates during apoptosis. Exper Cell Res 344:112–119

36. Model MA, Petruccelli JC (in press) Intracellular macromolecules in cell volume control and methods of their quantification. Curr Top Membr 81

37. Theillet FX, Binolfi A, Frembgen-Kesner T, Hingorani K, Sarkar M, Kyne C, Li C, Crowley PB, Gierasch L, Pielak GJ, Elcock AH, Gershenson A, Selenko P (2014) Physicochemical properties of cells and their effects on intrinsically disordered proteins (IDPs). Chem Rev 114:6661–6714

38. Ellis RJ (2001) Macromolecular crowding: obvious but underappreciated. Trends Biochem Sci 26:597–604

39. Benítez-Rangel E, López-Méndez MC, García L, Guerrero-Hernández A (2015) DIDS (4,4′-diisothiocyanatostilbene-2,2′-disulfonate) directly inhibits caspase activity in HeLa cell lysates. Cell Death Discov 1:15037

40. Liu AH, Cao YN, Liu HT, Zhang WW, Liu Y, Shi TW, Jia GL, Wang XM (2008) DIDS attenuates staurosporine-induced cardiomyocyte apoptosis by PI3K/Akt signaling pathway: activation of eNOS/NO and inhibition of Bax translocation. Cell Physiol Biochem 22:177–186

41. Doughty JM, Miller AL, Langton PD (1998) Non-specificity of chloride channel blockers in rat cerebral arteries: block of the L-type calcium channel. J Physiol 507:433–439

42. Liu K, Samuel M, Ho M, Harrison RK, Paslay JW (2010) NPPB structure-specifically activates TRPA1 channels. Biochem Pharmacol 80:113–121

43. Macias WL, McAteer JA, Tanner GA, Fritz AL, Armstrong WM (1992) NaCl transport by Madin Darby canine kidney cyst epithelial cells. Kidney Int 42:308–319